



# Enhanced leaf turnover and nitrogen recycling sustain CO<sub>2</sub> fertilization effect on tree-ring growth

Ying Guo<sup>1,2,7</sup>, Lin Zhang<sup>1,7</sup>, Liu Yang<sup>1,2</sup>, Wei Shen<sup>1</sup>, Yude Pan<sup>3</sup>, Ian J. Wright<sup>4,5</sup>, Yiqi Luo<sup>6</sup> and Tianxiang Luo<sup>1</sup>✉

**Whether increased photosynthates under elevated atmospheric CO<sub>2</sub> could translate into sustained biomass accumulation in forest trees remains uncertain. Here we demonstrate how tree radial growth is closely linked to litterfall dynamics, which enhances nitrogen recycling to support a sustained effect of CO<sub>2</sub> fertilization on tree-ring growth. Our ten-year observations in two alpine treeline forests indicated that annual (or seasonal) stem radial increments generally had a positive relationship with the previous year's (or season's) litterfall and its associated nitrogen return and resorption. Annual tree-ring width, annual litterfall and annual nitrogen return and resorption all showed an increasing trend during 2007–2017, and most of the variations were explained by elevated atmospheric CO<sub>2</sub> rather than climate change. Similar patterns were found in the longer time series of tree-ring width index from 1986–2017. The regional representativeness of our observed patterns was confirmed by the literature data of six other tree species at 11 treeline sites over the Tibetan Plateau. Enhanced nitrogen recycling through increased litterfall under elevated atmospheric CO<sub>2</sub> supports a general increasing trend of tree-ring growth in recent decades, especially in cold and nitrogen-poor environments.**

In boreal and alpine trees, it is highly debatable whether time series of tree-ring widths can provide a long-term record about responses of tree radial growth to elevated atmospheric CO<sub>2</sub> concentration (eCO<sub>2</sub>). It has been reported that eCO<sub>2</sub> may have a significant enhancement effect<sup>1–4</sup> or alternatively just a minor effect<sup>5,6</sup> on tree-ring growth. It is still difficult to quantify the extent to which eCO<sub>2</sub> fertilization may explain the increasing trend of tree-ring widths in recent decades, because changes in air temperature and atmospheric CO<sub>2</sub> are highly synchronized and there is lack of suitable data to effectively tease apart the underlying physiological mechanisms<sup>7–10</sup>. In most cases there are increases in both litterfall<sup>11–13</sup> and tree-ring increments<sup>14–17</sup> under CO<sub>2</sub>-enriched environments. However, it has been proposed that progressive nitrogen limitation under CO<sub>2</sub> enrichment may constrain the continuous response of tree-ring growth to eCO<sub>2</sub> unless nitrogen supply is enhanced from various sources<sup>7,9,18</sup>. Elevated CO<sub>2</sub> generally leads to increased photosynthesis<sup>7,19,20</sup>, which is expected to accelerate leaf turnover and nitrogen recycling because increased photosynthetic rates are typically associated with reduced leaf lifespan across species and ecosystems<sup>21,22</sup>. It is unknown whether there is a close linkage between litterfall and tree-ring growth, and if litterfall-enhanced N recycling plays a role in sustaining the effect of CO<sub>2</sub> fertilization on tree-ring growth. Such knowledge is critical for predicting responses of forest carbon and nitrogen cycles to global change.

At alpine treelines, the early growing season prior to summer solstice is the most important period for tree radial growth and leaf physiology<sup>23</sup>. Seasonal stem increment and photosynthetic capacity tend to peak around summer solstice<sup>24,25</sup>, which allows cold-limited trees sufficient time for completing secondary cell wall lignification before the winter. Low soil temperatures during the early growing season generally cause low soil nutrient availability,

which is another major constraint on tree growth<sup>26,27</sup>. The seasonal signals in leaves<sup>28,29</sup> may regulate leaf turnover to improve plant nitrogen use efficiency through reabsorbing nitrogen from senesced leaves<sup>30,31</sup>. There is evidence that seasonal stem increment typically shows a lagged positive relationship with litterfall, suggesting a likely linkage between stem growth and leaf turnover in treeline forests<sup>23</sup>. In a steady-state canopy system, leaf mass productivity is equal to the rate of leaf mass loss, and nitrogen uptake rate in green leaves is equal to nitrogen loss rate by litterfall and leaching<sup>30,31</sup>. The litterfall-induced nitrogen return and resorption may play an important role in regulating responses of tree-ring growth to changing environmental conditions, which may contribute to a higher sensitivity to eCO<sub>2</sub> than to warming. Here we hypothesize that tree radial growth generally has a lagged positive relationship with litterfall and its induced nitrogen return and resorption, and their interannual variations are mainly explained by eCO<sub>2</sub> rather than by warming, suggesting a sustained effect of eCO<sub>2</sub> fertilization on tree-ring growth in recent decades.

To test the hypothesis, we conducted ten-year observations (2007–2017) of seasonal stem radial increment, canopy litterfall and its induced nitrogen return (N-ret) and resorption (N-res) as well as climate factors at two alpine treelines in southeast Tibet. We also investigated the variation in tree-ring width index over a longer time period (1986–2017) across the two treeline species (*Abies georgei* var. *smithii* and *Juniperus saltuaria*). The time-series data (1986–2017) of monthly climatic factors and atmospheric CO<sub>2</sub> concentration were obtained from the Nyingchi weather station in southeast Tibet (~10 km from our study sites) and the Mauna Loa Observatory, Hawaii, respectively. We aimed to examine three key issues: (1) whether seasonal and annual stem increments typically show a lagged positive relationship with litterfall, N-ret and N-res

<sup>1</sup>Institute of Tibetan Plateau Research, Chinese Academy of Sciences, Beijing, China. <sup>2</sup>University of Chinese Academy of Sciences, Beijing, China. <sup>3</sup>USDA Forest Service, Northern Research Station, Durham, NH, USA. <sup>4</sup>Hawkesbury Institute for the Environment, Western Sydney University, Penrith, New South Wales, Australia. <sup>5</sup>Department of Biological Sciences, Macquarie University, North Ryde, New South Wales, Australia. <sup>6</sup>Center for Ecosystem Science and Society, Department of Biological Sciences, Northern Arizona University, Flagstaff, AZ, USA. <sup>7</sup>These authors contributed equally: Ying Guo, Lin Zhang. ✉e-mail: [luotx@itpcas.ac.cn](mailto:luotx@itpcas.ac.cn)

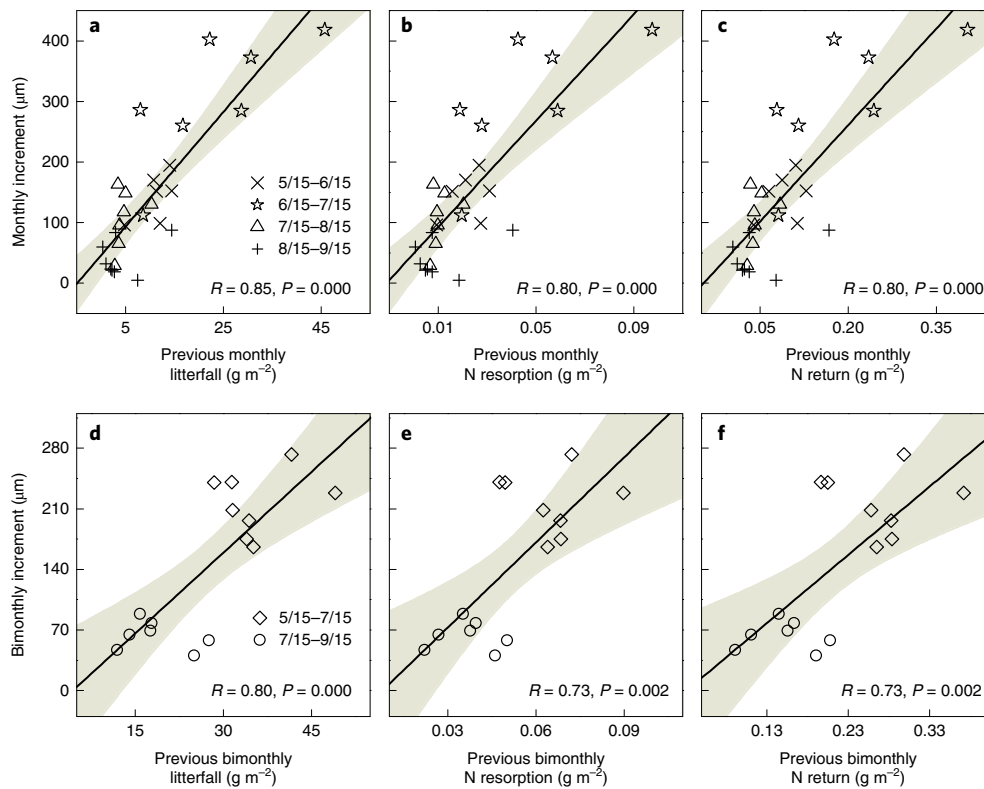


**Fig. 1 | Relationships of seasonal stem increment to previous season's litterfall and its induced N recycling at two alpine treelines during 2007-2017.** **a-c**, Monthly stem increments were positively correlated with previous monthly litterfall (**a**), N-res (**b**) and N-ret (**c**) in *A. georgei* var. *smithii* forest. **d-f**, Bimonthly stem increments were positively correlated with previous bimonthly litterfall (**d**), N-res (**e**) and N-ret (**f**) in *J. saltuaria* forest. The symbols are for seasonal stem increments. The relationships were tested using a simple linear model. The predicted mean (solid lines) is bounded by the 95% confidence intervals (shaded areas). The significance of correlation coefficient is estimated by two-tailed *t*-test with no adjustment for multiple comparisons.

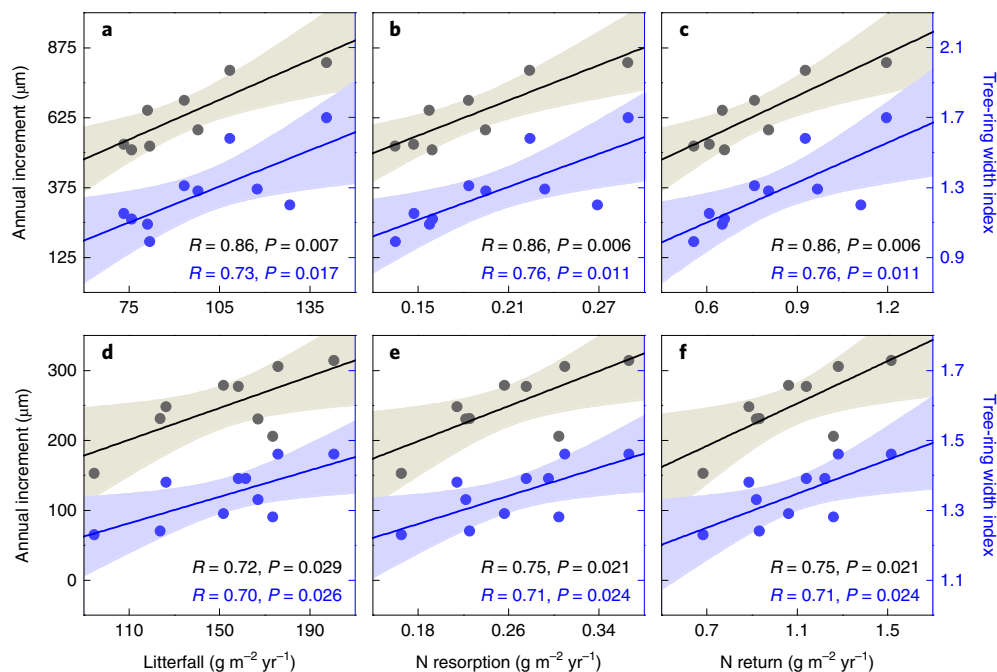


**Fig. 2 | Relationships of annual stem increment to previous year's litterfall and its induced N recycling at two alpine treelines during 2007-2017.** **a-c**, Annual stem increments were positively correlated with previous year's (from previous mid-June to current mid-June) litterfall (**a**), N-res (**b**) and N-ret (**c**) in *A. georgei* var. *smithii* forest. **d-f**, Annual stem increments were positively correlated with previous year's (from previous mid-June to current mid-June) litterfall (**d**), N-res (**e**) and N-ret (**f**) in *J. saltuaria* forest. Grey solid circles indicate annual stem increment by dendrometers and blue solid circles are for tree-ring width index by increment borers. The relationships were tested using a simple linear model. The predicted mean (solid lines) is bounded by the 95% confidence intervals (shaded areas). The significance of correlation coefficient is estimated by two-tailed *t*-test with no adjustment for multiple comparisons.

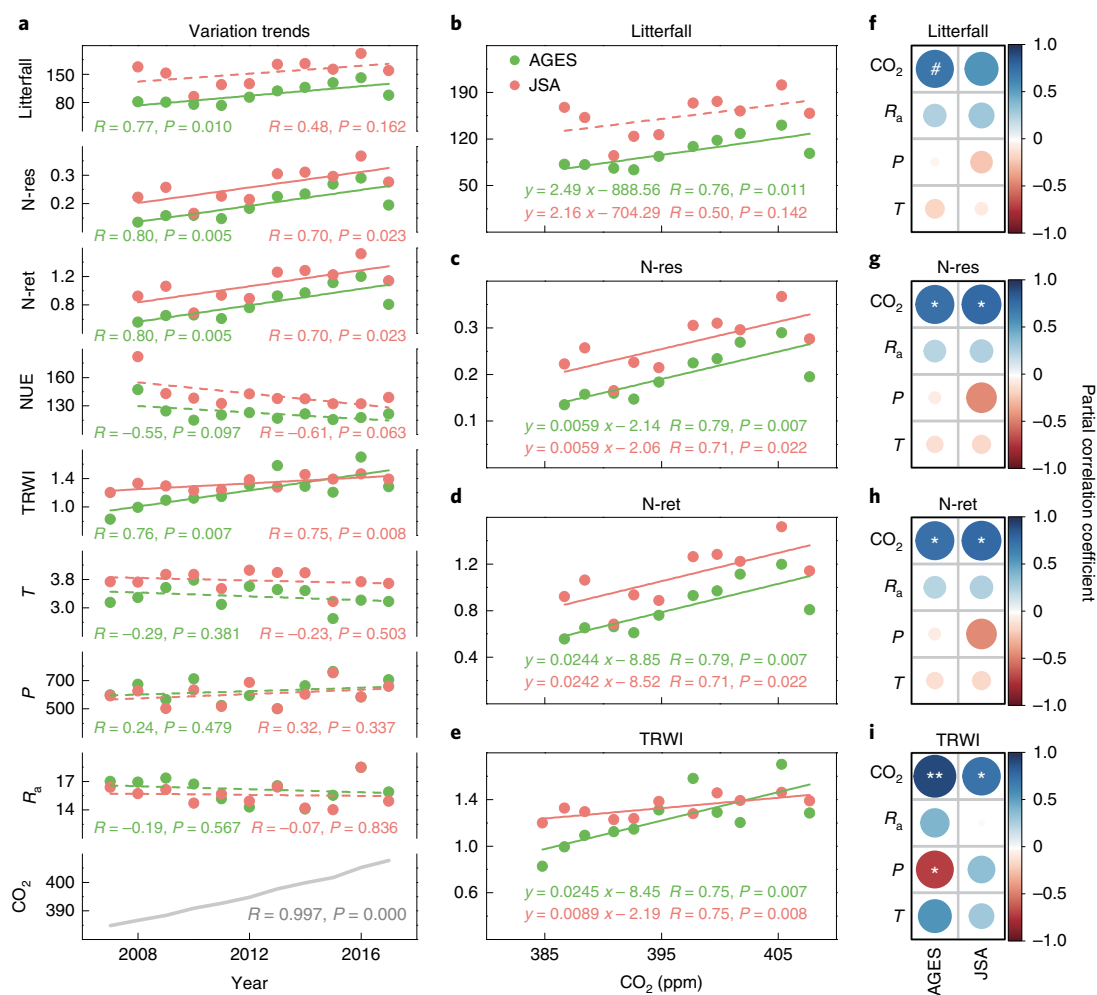


**Fig. 3 | Relative contributions of climatic factors and atmospheric  $CO_2$  to annual variations of litterfall, N recycling and tree-ring growth at two alpine treelines during 2007–2017.** **a**, A simple linear model was used for testing variation trends in annual litterfall ( $g\ m^{-2}\ yr^{-1}$ ), nitrogen resorption (N-res,  $g\ m^{-2}\ yr^{-1}$ ), nitrogen return (N-ret,  $g\ m^{-2}\ yr^{-1}$ ), nitrogen use efficiency (NUE,  $g\ DM\ g^{-1}$ ) and tree-ring width index (TRWI) for *A. georgei* var. *smithii* (AGES, green solid circles) and *J. saltuaria* (JSA, red solid circles), and the trends in climatic factors of growing season (May–August) mean minimum temperature (T,  $^{\circ}C$ ) and precipitation (P, mm) and solar radiation ( $R_a$ ,  $MJ\ m^{-2}\ d^{-1}$ ) observed at the two treelines, and in atmospheric  $CO_2$  concentration ( $CO_2$ , ppm) from Mauna Loa Observatory, Hawaii (<https://www.esrl.noaa.gov/gmd/ccgg/trends/>). **b–e**, A simple linear model was used for testing relationships of litterfall (**b**), N-res (**c**), N-ret (**d**) and TRWI (**e**) to atmospheric  $CO_2$  at both treelines. **f–i**, Partial correlation coefficients of multiple linear regressions for relationships of litterfall (**f**), N-res (**g**), N-ret (**h**) and TRWI (**i**) with climatic factors (T, P,  $R_a$ ) and atmospheric  $CO_2$  at both treelines; the partial correlation coefficients in different seasons and their exact P values are found in Supplementary Table 3. The significance of the correlation coefficient is estimated by two-tailed t-test with no adjustment for multiple comparisons. Significance level: # $P < 0.10$ , \* $P < 0.05$ , \*\* $P < 0.01$ .

across the two treeline stands; (2) whether annual tree-ring width, litterfall, N-ret and N-res all have a higher sensitivity to  $eCO_2$  than to the variability of temperature, precipitation and solar radiation during 2007–2017; and if so, (3) whether similar patterns are found in the longer time series of tree-ring width index during 1986–2017. We also assessed whether climatic factors and atmospheric  $CO_2$  have direct or indirect (via interactions with litterfall and N-ret/N-res) effects on tree radial growth using structural equation models. To test the regional representativeness of our observed patterns, we further examined the literature data of tree-ring widths for six other tree species at 11 treeline sites on the Tibetan Plateau (Supplementary Table 1).

## Results

**Relationship of stem increment with litterfall and N recycling.** During 2007–2017, monthly stem increments in *A. georgei* var. *smithii* (Fig. 1a–c) or bimonthly stem increments in *J. saltuaria*

(Fig. 1d–f) were positively correlated with previous monthly/bimonthly litterfall, N-res and N-ret. Also, annual stem increments and tree-ring width indices of *A. georgei* var. *smithii* (Fig. 2a–c) and *J. saltuaria* (Fig. 2d–f) generally showed a lagged positive relationship with annual litterfall, N-res and N-ret collected from previous mid-June to current mid-June (or from previous mid-May/mid-July to current mid-May/mid-July; Supplementary Table 2) during 2007–2017.

**Response factors of TRWI, litterfall, N-res and N-ret.** In response to the increase of atmospheric  $CO_2$  and insignificant changes in temperature, precipitation and solar radiation during 2007–2017, tree-ring width index (TRWI), annual litterfall, N-res and N-ret in both treeline forests typically indicated a significant increasing trend (except for litterfall in *J. saltuaria*, Fig. 3a). While nitrogen use efficiency (NUE, defined as the inverse of weighted average leaf-litter nitrogen concentration) showed a slight decreasing trend

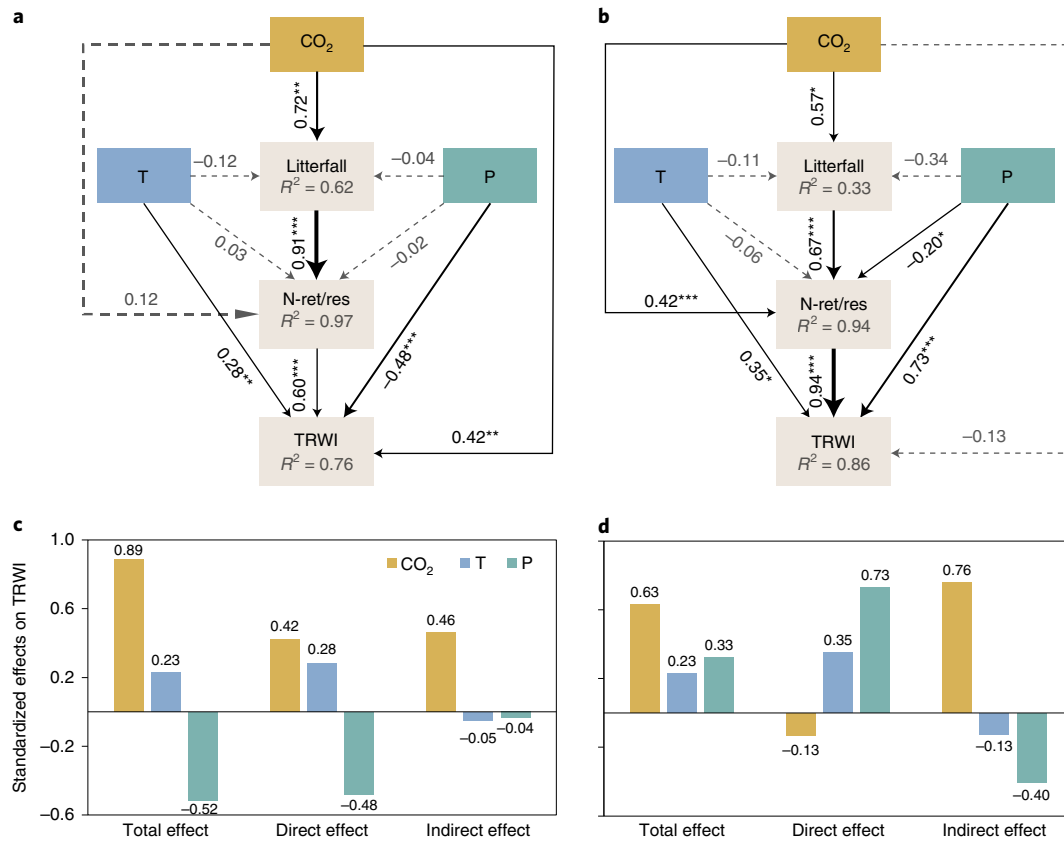


**Fig. 4 | Structural equation models quantifying direct effects of climatic factors and atmospheric CO<sub>2</sub> and their indirect effects through interactions with litterfall and N-ret/N-res on tree-ring width index at two alpine treelines during 2007–2017.** **a,c**, Standardized path coefficients (**a**) and the total, direct and indirect effects (**c**) of climatic factors and atmospheric CO<sub>2</sub> on TRWI in *A. georgei* var. *smithii* forest ( $\chi^2 = 0.310$ ,  $P = 0.578$ , CFI = 1.00, RMSEA = 0.000, AIC = 40.31). **b,d**, Standardized path coefficients (**b**) and the total, direct and indirect effects (**d**) of climatic factors and atmospheric CO<sub>2</sub> on TRWI in *J. saltuaria* forest ( $\chi^2 = 0.507$ ,  $P = 0.477$ , CFI = 1.00, RMSEA = 0.000, AIC = 40.51). Abbreviations of the measured variables are the same as in Fig. 3. Black solid arrows denote significant paths and arrow width indicates the strength of the relationship. Grey dashed arrows represent non-significant paths. The figures adjacent to arrows are for standardized path coefficients. R<sup>2</sup> value represents the proportion of variance explained for each dependent variable in the models. Significance level: \* $P < 0.05$ , \*\* $P < 0.01$ , \*\*\* $P < 0.001$ . The exact  $P$  values are found in Supplementary Table 4.

( $P < 0.10$ , Fig. 3a), there were significant increasing trends in mean and minimum leaf-litter nitrogen concentrations of *A. georgei* var. *smithii* and in mean and maximum leaf-litter nitrogen concentrations of *J. saltuaria* (Supplementary Fig. 1a). In general, TRWI, annual litterfall, N-res and N-ret all increased with eCO<sub>2</sub> (except for litterfall in *J. saltuaria*, Fig. 3b–e). Partial correlation analysis of multiple regression models indicated that eCO<sub>2</sub> was the dominant driver of variations in tree-ring width index, annual litterfall, N-res and N-ret, compared with minor effects of temperature, precipitation and solar radiation at both treelines (Fig. 3f–i and Supplementary Table 3). Similar patterns were found for variation in leaf-litter nitrogen concentrations across both treeline forests (Supplementary Fig. 1b–g).

Structural equation modelling revealed clear, indirect effects of eCO<sub>2</sub> on tree radial growth via positive interactions with annual litterfall and nitrogen return/resorption in both treeline forests (Fig. 4a,b and Supplementary Table 4). For *A. georgei* var. *smithii*, there was also a significant direct effect of eCO<sub>2</sub> on tree radial growth (Fig. 4a), and the standardized direct eCO<sub>2</sub> effect was similar in magnitude to the sum of indirect effects (Fig. 4c). For *J. saltuaria*, there was no direct effect of eCO<sub>2</sub> on tree radial growth (Fig. 4b), and the indirect effects of eCO<sub>2</sub> far outweighed the direct effect (Fig. 4d). For climatic factors, direct effects on tree radial growth were larger than indirect effects. Growing season mean minimum temperature had a direct positive effect on tree-ring

widths at both treelines (Fig. 4a,b). The direct precipitation effects on tree-ring width were negative in *A. georgei* var. *smithii* on the north-facing slope (Fig. 4a) but positive in *J. saltuaria* on the south-facing slope (Fig. 4b). In general, the total effect of eCO<sub>2</sub> was much higher than that of climate factors (Fig. 4c,d).

Over a longer time period (1986–2017), the TRWI and its ten-year moving averages generally showed significant increasing trends across the two treeline species in this study as well as six other tree species (at ten of 11 treeline sites) from the literature (Fig. 5a and Supplementary Fig. 2). Also, the long-term variations in tree-ring width indices (Fig. 5b) and their ten-year moving averages (Fig. 5c) of the eight treeline species (at 12 of 13 treeline sites) over the Tibetan Plateau were predominantly explained by eCO<sub>2</sub> rather than by climate change (more detailed information is found in Supplementary Table 5).

## Discussion

Elevated CO<sub>2</sub> generally leads to increased photosynthesis and reduced transpiration, both resulting in increased forest water use efficiency<sup>19</sup>. However, uncertainty remains over whether the increased photosynthates could translate into sustained biomass accumulation in forest trees<sup>7–9</sup>. Under free-air CO<sub>2</sub> enrichment (FACE), growth rates of temperate tree species may increase (for example, *Populus*<sup>15</sup>, *Pinus taeda*<sup>16</sup>, *Larix decidua*<sup>17</sup>) or vary little (for example, hardwood forest trees<sup>5</sup>, *Picea abies*<sup>6</sup>, *Pinus uncinata*<sup>17</sup>). Carbon allocation to different

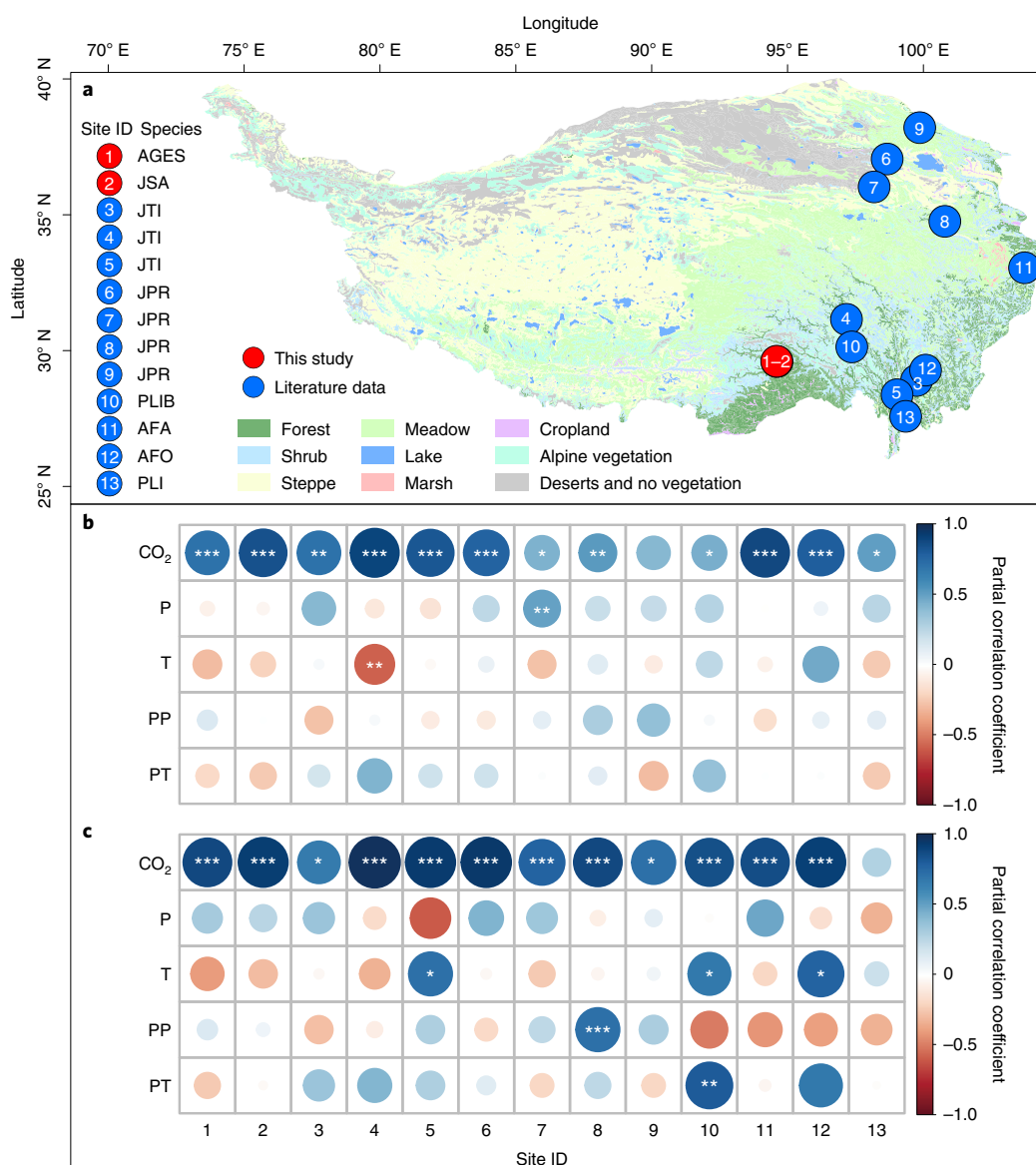


**Fig. 5 | Relative contributions of climatic factors and atmospheric CO<sub>2</sub> to annual variations of tree-ring width index (since 1986) across 8 tree species and 13 treeline sites on the Tibetan Plateau. a**, Spatial distribution of 13 tree-ring width chronologies. The background is the distribution map of vegetation types, which was drawn using ArcGIS 10.3 for Desktop with the vector data for Vegetation Atlas of China (1:1,000,000)<sup>50</sup>, available free online at <https://www.geodata.cn/>. Species abbreviations: AGES, *Abies georgei* var. *smithii*; JSA, *Juniperus saltuaria*; JTI, *Juniperus tibetica*; JPR, *Juniperus przewalskii*; PLIB, *Picea likiangensis* var. *balfouriana*; AFA, *Abies faxoniana*; AFO, *Abies forrestii*; PLI, *Picea likiangensis*. **b,c**, Partial correlation coefficients of multiple linear regression for relationships of tree-ring width indices (**b**, TRWI) and their ten-year moving averages (**c**) to previous and current years' early season (May–June) mean minimum temperatures (PT, T) and precipitation (PP, P), and atmospheric CO<sub>2</sub> concentration (CO<sub>2</sub>); the partial correlation coefficients between TRWI and climate factors in different seasons and their exact *P* values are found in Supplementary Tables 5 and 6. Detailed site information is found in Supplementary Table 1. The statistical significance is estimated by two-tailed *t*-test with no adjustment for multiple comparisons. Significance level: \**P* < 0.05, \*\**P* < 0.01, \*\*\**P* < 0.001.

pools (for example, wood or fine root) plays an important role in determining carbon cycling and the capacity of carbon accumulation by trees<sup>7,32</sup>. In addition, it has been suggested that long-term exposure to enriched CO<sub>2</sub> may lead to photosynthetic acclimation because non-structural carbohydrates may accumulate in leaves and then leaf nitrogen and rubisco contents may decline, which diminishes or restrains the eCO<sub>2</sub> fertilization effect on plant growth<sup>14</sup>. Furthermore, the increase of photosynthetic rate under eCO<sub>2</sub> may increase the demand for nitrogen, leading to progressive nitrogen limitation on plant photosynthesis and growth<sup>9,18</sup>. However, such ecophysiological mechanisms revealed from FACE experiments do not offer an explanation for the increasing trend of tree-ring widths

in recent decades observed in this study (Fig. 5 and Supplementary Fig. 2) and many previous reports (for example, *Populus tremuloides*<sup>1</sup>, *Fitzroya cupressoides*<sup>2</sup>, Norway spruce<sup>3</sup>, red spruce<sup>4</sup>). Stable carbon and oxygen isotopic records from tree rings generally indicate that stimulated leaf photosynthesis, rather than reduced stomatal conductance, is primarily responsible for the recent general increase in tree water use efficiency under eCO<sub>2</sub>, especially in areas with adequate water supply<sup>33,34</sup>. Even so, it is unclear whether and how eCO<sub>2</sub> may have continuously promoted the tree-ring growth of boreal and alpine trees in recent decades.

Leaf turnover and N recycling may play an important role in regulating tree growth response to eCO<sub>2</sub>, but these possibilities have

received little attention in previous studies. To conserve nitrogen resources, litterfall-induced N recycling is one of the most important strategies used by nearly all plant species<sup>30</sup>. Our ten-year observations revealed that elevated atmospheric CO<sub>2</sub> showed primarily an indirect enhancement effect on tree radial growth through increased litterfall and nitrogen return/resorption in the two treeline forests (Fig. 4). Annual nitrogen return by litterfall ranged from 0.56 to 1.52 g m<sup>-2</sup> yr<sup>-1</sup> in the two treeline forests (Fig. 3a), which was less than the nitrogen uptake rates measured in warm temperate forests (for example, 5.31 g m<sup>-2</sup> yr<sup>-1</sup> in aspen forests and 4.86 g m<sup>-2</sup> yr<sup>-1</sup> in pine forests<sup>35</sup>), probably due to low soil nitrogen availability at alpine treelines where temperature is much lower. The estimated nitrogen resorption (0.13–0.37 g m<sup>-2</sup> yr<sup>-1</sup>) was about 24% of the nitrogen return at both treelines. The litterfall-induced nitrogen return and resorption generally increased with eCO<sub>2</sub> (Fig. 3c,d), which was closely coupled with the increased stem radial growth in the two treeline forests (Figs. 1 and 2). In particular, the increased rates of annual nitrogen return by litterfall were ~2.43 g m<sup>-2</sup> yr<sup>-1</sup> per 100 ppm eCO<sub>2</sub> in both treeline forests (Fig. 3c,d), which was higher than the rates of annual nitrogen uptake by temperate trees under FACE environments (0.47–1.57 g m<sup>-2</sup> yr<sup>-1</sup> per 100 ppm eCO<sub>2</sub>)<sup>35</sup>. The significant increasing trend of mean leaf-litter nitrogen concentrations in the recent decade (Supplementary Fig. 1a) suggests an increase of nitrogen uptake by trees with an equal amount to the nitrogen loss by litterfall<sup>30,31</sup>. The slightly decreased NUE (Fig. 3a) was not correlated with tree radial growth in both treeline forests ( $P > 0.10$ ), which was consistent with previous reports<sup>35</sup>. Furthermore, tree-ring width index, annual litterfall, nitrogen return/resorption and leaf-litter nitrogen concentration all indicated a higher sensitivity to eCO<sub>2</sub> than to the variability of climatic factors (Figs. 3–5, Tables 3 and 4 and Supplementary Fig. 1), which is consistent with many previous studies<sup>3,4</sup>. Thus, the litterfall-enhanced nitrogen return and resorption can reduce the nitrogen limitation to plant growth under eCO<sub>2</sub>. Such a mechanism provides a new explanation for the general increasing trend of tree radial growth in recent decades observed in this study (Fig. 3a, Fig. 5 and Supplementary Fig. 2) and previous reports<sup>1–4</sup>.

Climate change impacts on tree radial growth varied with time periods and slope aspects (Figs. 3–5) because of variable patterns in precipitation change, snow cover and snow melting<sup>23</sup>. In water-limited forests, the decrease of stomatal conductance induced by eCO<sub>2</sub> can reduce water loss through transpiration and thus improve soil water availability<sup>36</sup>. However, severe stomatal closure due to intensified water stress caused by climate warming may also constrain leaf photosynthesis and subsequently tree growth<sup>8,37</sup>. This may explain the lack of response of tree radial growth to eCO<sub>2</sub> in some areas where annual precipitation is low<sup>8,37</sup> (site 9 in Fig. 5b). On the other hand, tree growth may vary little with eCO<sub>2</sub> when the increasing demand for nitrogen under rapid increase of atmospheric CO<sub>2</sub> exceeds the rate of N recycling from leaf turnover.

In temperate and boreal forests, <sup>13</sup>CO<sub>2</sub> pulse-labelling experiments have revealed that earlywood, the determinant of annual tree-ring width, contains both photosynthates produced in the previous summer and autumn and in the current spring<sup>38,39</sup>. This may explain why annual stem increment (tree-ring width index) generally had a close relationship with the last year's litter production and its related nitrogen return and resorption processed from the onset of previous growing season to the beginning of the current growing season (Fig. 2 and Supplementary Table 2). These findings further support an active carbon storage strategy taken by trees in harsh environments, which allows trees to cope with the asynchrony of supply and demand for carbon in the early growing season and to prepare for unpredictable disturbances such as freezing damage<sup>30,40</sup>. The findings also provide a basis for interpreting the positive relationship between TRWI and previous year (and/or current year) photosynthetic productivity found in many earlier

studies (for example, black spruce forest<sup>41</sup>, Norway spruce forest<sup>42</sup>, *Rhododendron* shrub<sup>43</sup>, Howland forest<sup>44</sup>).

In evergreen conifers, reduced leaf area index by shedding older leaves in the early growing season can improve light penetration into the canopy and then increase soil temperature, resulting in increases of soil nitrogen availability and canopy photosynthetic productivity<sup>31,45</sup>. Nitrogen reabsorbed from senescent leaves and photosynthates produced by mature leaves are primarily used for new leaf growth, and the developing leaves become carbon sources for secondary growth of stem and root later, when they are half-grown<sup>30,31,45</sup>. For evergreen conifers, 50–80 days are needed to construct a full-grown leaf (that is, 25–40 days for a half-grown leaf)<sup>21</sup>. This may explain why monthly (or bimonthly) stem increment was positively correlated with previous monthly (or bimonthly) litterfall and nitrogen resorption/return, with a delay of one to two months (Fig. 1).

In conclusion, our data support the hypotheses that there is a close linkage between leaf turnover and tree-ring growth, and that litterfall-enhanced nitrogen return and resorption can reduce the nitrogen limitation to plant growth under elevated atmospheric CO<sub>2</sub>. The findings offer a new explanation for the general increasing trend of tree-ring widths in recent decades that has been globally observed in temperate, boreal and alpine trees, and provide a new basis for detecting the long-term changes in forest litterfall and N recycling according to tree-ring width records. The revealed mechanisms for litterfall-accelerated N recycling and its link to the sustained effect of CO<sub>2</sub> fertilization on plant growth should be considered in terrestrial biogeochemical models.

## Methods

**Study sites.** This study was conducted on the north-facing and south-facing slopes of a U-shaped valley at the peak of the Sergyemla Mountains (29° 36' N, 94° 36' E) in southeast Tibet. Dominant tree species of both treelines are *Abies georgei* var. *smithii* on the north-facing slope and *Juniperus saltuaria* on the south-facing slope. Along both slopes the vegetation changes from sub-alpine and treeline forests (tree height >4 m and canopy coverage >40%) to an open mosaic of alpine shrublands and grasslands. In August 2005, two long-term observing plots (50 × 50 m<sup>2</sup>) were established in both treeline forests. The stand basal area and mean tree height (mean ± s.d.) were 39.7 m<sup>2</sup> ha<sup>-1</sup> and 10.2 ± 1.0 m for *A. georgei* var. *smithii* and 39.8 m<sup>2</sup> ha<sup>-1</sup> and 7.6 ± 0.5 m for *J. saltuaria*. Four automatic weather stations (HL20, Jauntering Inc., Taiwan) were installed in treeline forests of *A. georgei* var. *smithii* (4,320 m) and *J. saltuaria* (4,425 m) and above both treelines. During 2006–2017, annual mean air temperature was 0.6 °C and 1.1 °C in treeline forests of *A. georgei* var. *smithii* and *J. saltuaria*, respectively. The growing season precipitation (May–August) was similar between north-facing and south-facing slopes (769 mm and 745 mm, respectively). Daily mean soil volume moisture content during the growing season was typically >35% on both slopes. Spring soil warming date (when soil temperatures began to be continuously above 0 °C) was 20–30 days earlier on the south-facing slope than on the north-facing slope.

**Litterfall and related nitrogen return and resorption.** In each of the treeline forests, five 1.5 × 0.5 m<sup>2</sup> litterfall traps were randomly installed in mid-August 2006. Monthly litterfall (including dead leaves and twigs) was collected every mid-month from May to October, and the litterfall accumulated after the previous October was collected in mid-April or mid-May. The litterfall was separated into needles, twigs, cones, barks and others. The separated components were oven-dried at 70 °C for approximately 48 hours and then weighed. As the N recycling largely occurs from senescent leaves, the data of needle litterfall in *A. georgei* var. *smithii* and scale-leaf twig litterfall in *J. saltuaria* were used for all analyses in this study. The leaf-litter nitrogen concentration was analysed by the Kjeldahl method.

Given that leaf mass production is equal to leaf mass loss (litterfall), and nitrogen uptake in green leaves is approximate to nitrogen return by litterfall in a steady-state canopy system<sup>30,31</sup>, the monthly nitrogen return (N-ret, g m<sup>-2</sup>) was calculated as:

$$\text{N-ret} = N_{\text{litter}} \times M_{\text{litter}}/100 \quad (1)$$

where  $N_{\text{litter}}$  is the leaf-litter nitrogen concentration (%) and  $M_{\text{litter}}$  is the dry mass of monthly leaf litterfall (g m<sup>-2</sup>). Also, the monthly nitrogen resorption (N-res, g m<sup>-2</sup>) was calculated as:

$$\text{N-res} = (N_{\text{green}} - N_{\text{litter}}) \times M_{\text{litter}}/100 \quad (2)$$

where  $N_{\text{green}}$  is the nitrogen concentration of green leaves (%). Because of difficulty in seasonal destructive sampling of canopy leaves in long-term observations,  $N_{\text{green}}$

was estimated from  $N_{\text{litter}}$  using a global empirical model ( $N_{\text{litter}} = 0.60N_{\text{green}}$ )<sup>46</sup> with a mass loss correction factor (MLCF, that is, the ratio of leaf litter mass to green leaf mass)<sup>47</sup>:

$$N_{\text{green}} = (N_{\text{litter}}/\text{MLCF})/0.60 \quad (3)$$

To correct the intrinsic underestimation of nitrogen resorption due to the mass loss and the change of measurement basis during leaf senescence, the MLCF of 0.745 for conifers was used as in Vergutz et al.<sup>47</sup>. To validate equation (3), we measured nitrogen concentrations of green leaves from the canopy and dead leaves from litter traps for each of five individual trees at *A. georgei* var. *smithii* treeline once every mid-month during May and September 2017. The estimated  $N_{\text{green}}$  using equation (3) was highly correlated with the observed values, being close to a one-to-one relationship ( $R^2 = 0.36$ ,  $P < 0.001$ , slope = 0.88; Supplementary Fig. 3).

Assuming that carbohydrates used for tree-ring growth are mainly from the reserves stored since the previous growing season and the concurrent photosynthates<sup>38,39</sup>, annual litterfall and annual nitrogen resorption and return were calculated as the sum of seasonal measurements from previous mid-June to current mid-June during 2007–2017. NUE was estimated as the inverse of the monthly litterfall-weighted average leaf-litter nitrogen concentration because the ratio of biomass production to nitrogen uptake is equal to the ratio of litterfall to nitrogen loss<sup>30,31</sup>.

**Stem radial increment with dendrometers.** In August 2005, eight mature and healthy trees at each of the two treeline sites were selected and mounted with automatic dendrometers of diameter and circumference (including 2 DD and 6 DC dendrometers, Ecomatik, Munich, Germany) at breast height to continuously monitor stem radial growth. The monitored trees of *A. georgei* var. *smithii* and *J. saltuaria* had an average height of  $9.6 \pm 1.8$  m and  $8.6 \pm 0.9$  m, diameter at breast height (DBH) of  $37.2 \pm 14.0$  cm and  $22.4 \pm 3.1$  cm, and stem age of  $188 \pm 61$  yr and  $207 \pm 24$  yr, respectively. Raw data were recorded hourly by a HL20 data logger (Jauntinger Inc.). The data measured by DD and DC types of dendrometers were divided by 2 and  $2\pi$ , respectively, to obtain the stem increment in radius. Because the data loggers were broken in 2007, we examined the data recorded during 2008–2017 in this study. Also, the data of 2014–2015 for *A. georgei* var. *smithii* and 2015 for *J. saltuaria* were lost because of sensor failure. Thus, there were eight and nine years of dendrometer data for *A. georgei* var. *smithii* and *J. saltuaria*, respectively.

Weekly stem radial increment was calculated as the difference of daily maximum values between the consecutive seventh day and the first day for each tree, year and species according to the method described by Rossi et al.<sup>24</sup>. Monthly stem increment was calculated as the sum of weekly increments within a month consistent with the sampling time of monthly litterfall. For the slow-growing *J. saltuaria*, bimonthly stem increment was calculated as the sum of two consecutive monthly increments. Annual stem increment was calculated as the sum of weekly increments over the growing season. Luo et al.<sup>23</sup> demonstrated that annual stem increments measured by dendrometers positively correlated well with the tree-ring widths of monitored trees, indicating that tree-ring growth signals can be extracted from dendrometer data. The average stem increment weighted by DBH of each monitored tree was related to the stand-level measurement of litterfall. Detailed information on the calculation method and the definition of onset and ending dates of stem radial increment is found in Luo et al.<sup>23</sup>.

**Tree-ring width chronologies and related climate data.** In October 2016, two tree-ring cores at breast height were sampled with an increment borer (Haglöf, Sweden) for each of 30 trees (including the eight monitored trees with dendrometers) in each of both treeline species. In October 2017, we further collected additional two cores for each of the eight monitored trees with dendrometers. The cores were processed following standard dendrochronological practices and annual ring width was measured with a resolution of 0.01 mm. After performing the cross-dating check by using the COFECHA program<sup>48</sup>, the raw data of the 76 tree-ring width series were transformed into indices by fitting a negative exponential function using the ARSTAN program<sup>49</sup>.

The ten-year climate data (2007–2017) of monthly mean minimum temperature, precipitation and solar radiation were obtained from the automatic weather stations at the two treelines in the Sergyemla Mountains. The climate data for a longer time period (1986–2017) were obtained from Nyingchi weather station at 3,000 m, ~10 km from our study sites. The time-series data (1986–2017) of atmospheric CO<sub>2</sub> concentration were obtained from Mauna Loa Observatory, Hawaii (<https://www.esrl.noaa.gov/gmd/ccgg/trends/>).

To test the generality of our observed data in the Sergyemla Mountains, we further collected the literature data of tree-ring width chronologies for six other species at 11 treeline sites over the Tibetan Plateau, which were obtained from the published papers and the International Tree-Ring Data Bank, available online at the website (<https://www.ncdc.noaa.gov/data-access/paleoclimatology-data/datasets/tree-ring>) (Supplementary Table 1). The time-series data of monthly mean minimum temperature and monthly precipitations at weather stations near the 11 sampling sites were obtained from the China Meteorological Data Service Centre (<http://data.cma.cn/data/detail/dataCode/A.0012.0001>).

**Data analysis.** A simple linear model was used for examining the variation trends in annual litterfall, N-ret, N-res, NUE and TRWI, as well as climatic factors (growing season mean minimum temperature, precipitation and solar radiation) and atmospheric CO<sub>2</sub> concentration, and for testing the relationships of seasonal/annual stem increment with seasonal/annual litterfall and its associated nitrogen resorption and return during 2007–2017.

Partial correlation analysis of multiple linear regression was used for assessing the relative importance of the current year's seasonal mean minimum temperature (T), precipitation (P), solar radiation (R<sub>s</sub>) and atmospheric CO<sub>2</sub> (CO<sub>2</sub>), as well as the previous year's seasonal mean minimum temperature (PT), precipitation (PP), solar radiation (PR<sub>s</sub>) and atmospheric CO<sub>2</sub> (PCO<sub>2</sub>) in determining the variations of annual litterfall, N-ret, N-res and TRWI in the two treeline forests during 2007–2017. Climatic variables and atmospheric CO<sub>2</sub> in different periods, including the early season (May–June, April–June), summer (June–August), the whole growing season (May–August, April–September) and the year, were inputted into the above regression models, respectively. To verify our ten-year observed data, partial correlation analysis was further performed to examine whether the tree-ring width chronologies in recent decades (since 1986) across eight tree species and 13 treeline sites on the Tibetan Plateau collected from this study and the literature also show similar patterns associated with climatic factors and atmospheric CO<sub>2</sub>. We further calculated ten-year moving averages of the 30-year data for tree-ring width indices, climatic factors and atmospheric CO<sub>2</sub> concentration across the eight tree species and the 13 treeline sites, and then performed the partial correlation analysis.

In addition, structural equation modelling was used to quantify direct effects of climatic factors and atmospheric CO<sub>2</sub> and their indirect effects through interactions with litterfall and nitrogen return/resorption on TRWI during 2007–2017. Based on the theoretical knowledge of the major factors controlling annual variation of TRWI, an a priori conceptual model was developed to relate climatic factors (T, P), atmospheric CO<sub>2</sub>, annual litterfall and N-ret/N-res to TRWI. Maximum-likelihood estimation was used to obtain the path coefficients. The  $\chi^2$  goodness-of-fit test ( $P < 0.05$  indicated a poor fit), comparative fit index (CFI), root mean square error of approximation (RMSEA) and Akaike information criterion (AIC) were used to test whether the model was a reasonable explanation of the observed pattern. Structural equation models were constructed by the AMOS v.24.0 package of the SPSS statistical software (SPSS Inc.).

All statistical analyses were performed using SPSS v.18.0 (SPSS Inc.). The map was drawn by ArcGIS v.10.3 for Desktop (Environmental Systems Research Institute, Inc.). All significant differences were taken at  $P < 0.05$ .

**Reporting summary.** Further information on research design is available in the Nature Research Reporting Summary linked to this article.

## Data availability

The tree-ring width chronologies collected from the International Tree-Ring Data Bank are available at <https://www.ncdc.noaa.gov/data-access/paleoclimatology-data/datasets/tree-ring>. The time-series data of atmospheric CO<sub>2</sub> concentration were obtained from <https://www.esrl.noaa.gov/gmd/ccgg/trends/>. The time-series data of monthly climatic factors at weather stations were obtained from <http://data.cma.cn/data/detail/dataCode/A.0012.0001>. All observed data in this study are provided in this article and its associated supplementary information.

Received: 10 December 2021; Accepted: 24 May 2022;

Published online: 11 July 2022

## References

- Cole, C. T., Anderson, J. E., Lindroth, R. L. & Waller, D. M. Rising concentrations of atmospheric CO<sub>2</sub> have increased growth in natural stands of quaking aspen (*Populus tremuloides*). *Glob. Change Biol.* **16**, 2186–2197 (2010).
- Urrutia-Jalabert, R. et al. Increased water use efficiency but contrasting tree growth patterns in *Fitzroya cupressoides* forests of southern Chile during recent decades. *J. Geophys. Res. Biogeosci.* **120**, 2505–2524 (2015).
- Cienciala, E. et al. Increased spruce tree growth in Central Europe since 1960s. *Sci. Total Environ.* **619–620**, 1637–1647 (2018).
- Mathias, J. M. & Thomas, R. B. Disentangling the effects of acidic air pollution, atmospheric CO<sub>2</sub>, and climate change on recent growth of red spruce trees in the Central Appalachian Mountains. *Glob. Change Biol.* **24**, 3938–3953 (2018).
- Körner, C. et al. Carbon flux and growth in mature deciduous forest trees exposed to elevated CO<sub>2</sub>. *Science* **309**, 1360–1362 (2005).
- Klein, T. et al. Growth and carbon relations of mature *Picea abies* trees under 5 years of free-air CO<sub>2</sub> enrichment. *J. Ecol.* **104**, 1720–1733 (2016).
- Norby, R. J. & Zak, D. R. Ecological lessons from free-air CO<sub>2</sub> enrichment (FACE) experiments. *Annu. Rev. Ecol. Syst.* **42**, 181–203 (2011).
- Peñuelas, J., Canadell, J. G. & Ogaya, R. Increased water-use efficiency during the 20th century did not translate into enhanced tree growth. *Glob. Ecol. Biogeogr.* **20**, 597–608 (2011).

9. IPCC. *Climate Change 2013: The Physical Science Basis* (eds Stocker, T. F. et al.) (Cambridge Univ. Press, 2013).
10. Dong, N. et al. Rising CO<sub>2</sub> and warming reduce global canopy demand for nitrogen. *New Phytol.* <https://doi.org/10.1111/nph.18076> (2022).
11. Finzi, A. C., Allen, A. S., DeLucia, E. H., Ellsworth, D. S. & Schlesinger, W. H. Forest litter production, chemistry, and decomposition following two years of free-air CO<sub>2</sub> enrichment. *Ecology* **82**, 470–484 (2001).
12. Liberloo, M. et al. Elevated CO<sub>2</sub> concentration, fertilization and their interaction: growth stimulation in a short-rotation poplar coppice (EUROFACE). *Tree Physiol.* **25**, 179–189 (2005).
13. Hungate, B. A. et al. Nitrogen cycling during seven years of atmospheric CO<sub>2</sub> enrichment in a scrub oak woodland. *Ecology* **87**, 26–40 (2006).
14. Ainsworth, E. A. & Long, S. P. What have we learned from 15 years of free-air CO<sub>2</sub> enrichment (FACE)? A meta-analytic review of the responses of photosynthesis, canopy properties and plant production to rising CO<sub>2</sub>. *New Phytol.* **165**, 351–372 (2005).
15. Liberloo, M. et al. Coppicing shifts CO<sub>2</sub> stimulation of poplar productivity to above-ground pools: a synthesis of leaf to stand level results from the POP/EUROFACE experiment. *New Phytol.* **182**, 331–346 (2009).
16. McCarthy, H. R. et al. Re-assessment of plant carbon dynamics at the Duke free-air CO<sub>2</sub> enrichment site: interactions of atmospheric [CO<sub>2</sub>] with nitrogen and water availability over stand development. *New Phytol.* **185**, 514–528 (2010).
17. Dawes, M. A. et al. Species-specific tree growth responses to 9 years of CO<sub>2</sub> enrichment at the alpine treeline. *J. Ecol.* **99**, 383–394 (2011).
18. Luo, Y. Q. et al. Progressive nitrogen limitation of ecosystem responses to rising atmospheric carbon dioxide. *Bioscience* **54**, 731–739 (2004).
19. Keenan, T. F. et al. Increase in forest water-use efficiency as atmospheric carbon dioxide concentrations rise. *Nature* **499**, 324–327 (2013).
20. Luo, Y. Q., Hui, D. F. & Zhang, D. Q. Elevated CO<sub>2</sub> stimulates net accumulations of carbon and nitrogen in land ecosystems: a meta-analysis. *Ecology* **87**, 53–63 (2006).
21. Kikuzawa, K. A cost-benefit analysis of leaf habit and leaf longevity of trees and their geographical pattern. *Am. Nat.* **138**, 1250–1263 (1991).
22. Wright, I. J. et al. The worldwide leaf economics spectrum. *Nature* **428**, 821–827 (2004).
23. Luo, T. X. et al. Summer solstice marks a seasonal shift in temperature sensitivity of stem growth and nitrogen-use efficiency in cold-limited forests. *Agric. For. Meteorol.* **248**, 469–478 (2018).
24. Rossi, S. et al. Conifers in cold environments synchronize maximum growth rate of tree-ring formation with day length. *New Phytol.* **170**, 301–310 (2006).
25. Bauerle, W. L. et al. Photoperiodic regulation of the seasonal pattern of photosynthetic capacity and the implications for carbon cycling. *Proc. Natl Acad. Sci. USA* **109**, 8612–8617 (2012).
26. Jarvis, P. & Linder, S. Constraints to growth of boreal forests. *Nature* **405**, 904–905 (2000).
27. Sullivan, P. F., Ellison, S. B., McNown, R. W., Brownlee, A. H. & Sveinbjörnsson, B. Evidence of soil nutrient availability as the proximate constraint on growth of treeline trees in northwest Alaska. *Ecology* **96**, 716–727 (2015).
28. Dodd, A. N. et al. Plant circadian clocks increase photosynthesis, growth, survival, and competitive advantage. *Science* **309**, 630–633 (2005).
29. Jackson, S. D. Plant responses to photoperiod. *New Phytol.* **181**, 517–531 (2009).
30. Chapin III, F. S., Matson, P. A. & Mooney, H. A. *Principles of Terrestrial Ecosystem Ecology* (Springer-Verlag, 2002).
31. Hikosaka, K. Leaf canopy as a dynamic system: ecophysiology and optimality in leaf turnover. *Ann. Bot.* **95**, 521–533 (2005).
32. Jiang, M. K. et al. The fate of carbon in a mature forest under carbon dioxide enrichment. *Nature* **580**, 227–231 (2020).
33. Guerrieri, R. et al. Disentangling the role of photosynthesis and stomatal conductance on rising forest water-use efficiency. *Proc. Natl Acad. Sci. USA* **116**, 16909–16914 (2019).
34. Mathias, J. M. & Thomas, R. B. Global tree intrinsic water use efficiency is enhanced by increased atmospheric CO<sub>2</sub> and modulated by climate and plant functional types. *Proc. Natl Acad. Sci. USA* **118**, e2014286118 (2021).
35. Finzi, A. C. et al. Increases in nitrogen uptake rather than nitrogen-use efficiency support higher rates of temperate forest productivity under elevated CO<sub>2</sub>. *Proc. Natl Acad. Sci. USA* **104**, 14014–14019 (2007).
36. Soulé, P. T. & Knapp, P. A. Radial growth rate increases in naturally occurring ponderosa pine trees: a late-20th century CO<sub>2</sub> fertilization effect? *New Phytol.* **171**, 379–390 (2006).
37. Linares, J. C. & Camarero, J. J. From pattern to process: linking intrinsic water-use efficiency to drought-induced forest decline. *Glob. Change Biol.* **18**, 1000–1015 (2012).
38. Kagawa, A., Sugimoto, A. & Maximov, T. C. <sup>13</sup>C<sub>2</sub> pulse-labelling of photoassimilates reveals carbon allocation within and between tree rings. *Plant Cell Environ.* **29**, 1571–1584 (2006).
39. Epron, D. et al. Pulse-labelling trees to study carbon allocation dynamics: a review of methods, current knowledge and future prospects. *Tree Physiol.* **32**, 776–798 (2012).
40. Wiley, E. & Helliker, B. A re-evaluation of carbon storage in trees lends greater support for carbon limitation to growth. *New Phytol.* **195**, 285–289 (2012).
41. Rocha, A. V., Goulsten, M. L., Dunn, A. L. & Wofsy, S. C. On linking interannual tree ring variability with observations of whole-forest CO<sub>2</sub> flux. *Glob. Change Biol.* **12**, 1378–1389 (2006).
42. Zweifel, R. et al. Link between continuous stem radius changes and net ecosystem productivity of a subalpine Norway spruce forest in the Swiss Alps. *New Phytol.* **187**, 819–830 (2010).
43. Kong, G. Q., Luo, T. X., Liu, X. S., Zhang, L. & Liang, E. Y. Annual ring widths are good predictors of changes in net primary productivity of alpine *Rhododendron* shrubs in the Sergyemla Mountains, southeast Tibet. *Plant Ecol.* **213**, 1843–1855 (2012).
44. Teets, A. et al. Linking annual tree growth with eddy-flux measures of net ecosystem productivity across twenty years of observation in a mixed conifer forest. *Agric. For. Meteorol.* **249**, 479–487 (2018).
45. Luo, T. X., Li, M. C. & Luo, J. Seasonal variations in leaf δ<sup>13</sup>C and nitrogen associated with foliage turnover and carbon gain for a wet subalpine fir forest in the Gongga Mountains, eastern Tibetan Plateau. *Ecol. Res.* **26**, 253–263 (2011).
46. Kobe, R. K., Lepczyk, C. A. & Iyer, M. Resorption efficiency decreases with increasing green leaf nutrients in a global data set. *Ecology* **86**, 2780–2792 (2005).
47. Vergutz, L., Manzoni, S., Porporato, A., Novais, R. F. & Jackson, R. B. Global resorption efficiencies and concentrations of carbon and nutrients in leaves of terrestrial plants. *Ecol. Monogr.* **82**, 205–220 (2012).
48. Holmes, R. L. Computer-assisted quality control in tree-ring dating and measurement. *Tree-Ring Bull.* **43**, 69–78 (1983).
49. Cook, E. R. & Kairiukstis, L. A. *Methods of Dendrochronology: Applications in the Environmental Sciences* (Kluwer Academic Publishers, 1990).
50. Editorial Board of Vegetation Map of China, Chinese Academy of Sciences. *Vegetation Atlas of China* (Science Press, 2001).

## Acknowledgements

We thank X. S. Liu for his help with the observation of stem radial increment and the Southeast Tibet Station for Alpine Environment Observation and Research, Chinese Academy of Sciences, for help in the fieldwork. This work was funded by the Second Tibetan Plateau Scientific Expedition and Research Programme (grant no. 2019QZKK0106) and the National Natural Science Foundation of China (grant nos. 41830649 and 41571046).

## Author contributions

T.L. designed the experiment. Y.G., L.Z., L.Y. and W.S. conducted the experiment. Y.G., L.Z., T.L., Y.P., I.J.W. and Y.L. analysed the data. Y.G., L.Z. and T.L. wrote the manuscript. Y.P., I.J.W. and Y.L. revised the manuscript.

## Competing interests

The authors declare no competing interests.

## Additional information

**Supplementary information** The online version contains supplementary material available at <https://doi.org/10.1038/s41559-022-01811-1>.

**Correspondence and requests for materials** should be addressed to Tianxiang Luo.

**Peer review information** *Nature Ecology & Evolution* thanks Flurin Babst and the other, anonymous, reviewer(s) for their contribution to the peer review of this work.

**Reprints and permissions information** is available at [www.nature.com/reprints](http://www.nature.com/reprints).

**Publisher's note** Springer Nature remains neutral with regard to jurisdictional claims in published maps and institutional affiliations.

© The Author(s), under exclusive licence to Springer Nature Limited 2022



## Reporting Summary

Nature Portfolio wishes to improve the reproducibility of the work that we publish. This form provides structure for consistency and transparency in reporting. For further information on Nature Portfolio policies, see our [Editorial Policies](#) and the [Editorial Policy Checklist](#).

### Statistics

For all statistical analyses, confirm that the following items are present in the figure legend, table legend, main text, or Methods section.

n/a Confirmed

- |                                     |                                     |  |
|-------------------------------------|-------------------------------------|--|
| <input type="checkbox"/>            | <input checked="" type="checkbox"/> | The exact sample size ( $n$ ) for each experimental group/condition, given as a discrete number and unit of measurement  |
| <input type="checkbox"/>            | <input checked="" type="checkbox"/> | A statement on whether measurements were taken from distinct samples or whether the same sample was measured repeatedly  |
| <input type="checkbox"/>            | <input checked="" type="checkbox"/> | The statistical test(s) used AND whether they are one- or two-sided<br><i>Only common tests should be described solely by name; describe more complex techniques in the Methods section.</i>   |
| <input checked="" type="checkbox"/> | <input type="checkbox"/>            | A description of all covariates tested   |
| <input type="checkbox"/>            | <input checked="" type="checkbox"/> | A description of any assumptions or corrections, such as tests of normality and adjustment for multiple comparisons  |
| <input type="checkbox"/>            | <input checked="" type="checkbox"/> | A full description of the statistical parameters including central tendency (e.g. means) or other basic estimates (e.g. regression coefficient) AND variation (e.g. standard deviation) or associated estimates of uncertainty (e.g. confidence intervals) |
| <input type="checkbox"/>            | <input checked="" type="checkbox"/> | For null hypothesis testing, the test statistic (e.g. $F$ , $t$ , $r$ ) with confidence intervals, effect sizes, degrees of freedom and $P$ value noted<br><i>Give <math>P</math> values as exact values whenever suitable.</i>                            |
| <input checked="" type="checkbox"/> | <input type="checkbox"/>            | For Bayesian analysis, information on the choice of priors and Markov chain Monte Carlo settings   |
| <input checked="" type="checkbox"/> | <input type="checkbox"/>            | For hierarchical and complex designs, identification of the appropriate level for tests and full reporting of outcomes   |
| <input type="checkbox"/>            | <input checked="" type="checkbox"/> | Estimates of effect sizes (e.g. Cohen's $d$ , Pearson's $r$ ), indicating how they were calculated   |

*Our web collection on [statistics for biologists](#) contains articles on many of the points above.*

### Software and code

Policy information about [availability of computer code](#)

Data collection No software was used.

Data analysis All statistical analyses were performed using the SPSS 18.0 for Windows (SPSS Inc., Chicago, Illinois, USA). The map was drawn by ArcGIS 10.3 for Desktop (Environmental Systems Research Institute, Inc., RedLands, California, USA).

For manuscripts utilizing custom algorithms or software that are central to the research but not yet described in published literature, software must be made available to editors and reviewers. We strongly encourage code deposition in a community repository (e.g. GitHub). See the Nature Portfolio [guidelines for submitting code & software](#) for further information.

### Data

Policy information about [availability of data](#)

All manuscripts must include a [data availability statement](#). This statement should provide the following information, where applicable:

- Accession codes, unique identifiers, or web links for publicly available datasets
- A description of any restrictions on data availability
- For clinical datasets or third party data, please ensure that the statement adheres to our [policy](#)

All data generated or analysed during this study are included in this manuscript and its supplementary information files.

## Field-specific reporting

Please select the one below that is the best fit for your research. If you are not sure, read the appropriate sections before making your selection.

Life sciences  Behavioural & social sciences  Ecological, evolutionary & environmental sciences

For a reference copy of the document with all sections, see [nature.com/documents/nr-reporting-summary-flat.pdf](https://www.nature.com/documents/nr-reporting-summary-flat.pdf)

## Ecological, evolutionary & environmental sciences study design

All studies must disclose on these points even when the disclosure is negative.

Study description	We demonstrated how tree-ring width growth is closely linked to litterfall dynamics and how litterfall-enhanced nitrogen recycling supports a sustained effect of CO <sub>2</sub> fertilization on tree-ring growth, based on our 10-year observed data at two alpine treeline sites.
Research sample	This study was conducted on the north-facing and south-facing slopes of a U-shaped valley at the peak of the Sergyemla Mountains (29°36'N, 94°36'E) in southeast Tibet. Dominant tree species of both treelines are <i>Abies georgei</i> var. <i>smithii</i> on the north-facing slope and <i>Juniperus saltuaria</i> on the south-facing slope. Along both slopes the vegetation changes from sub-alpine and treeline forests (tree height > 4 m and canopy coverage >40%) to open mosaic of alpine shrublands and grasslands. In August 2005, two long-term observing plots (50 × 50 m) were established in both treeline forests.
Sampling strategy	We conducted 10-year observations (2007-2017) of seasonal stem radial increment, canopy litterfall and its induced nitrogen return and resorption, as well as climate factors at two alpine treelines in southeast Tibet. We also investigated the variation of tree-ring width growth over a longer time period (1986-2017) across the two treeline species ( <i>Abies georgei</i> var. <i>smithii</i> and <i>Juniperus saltuaria</i> ). The time series data (1986-2017) of monthly climatic factors and atmospheric CO <sub>2</sub> concentration were obtained from the Nyingchi weather station in southeast Tibet (ca. 10 km from our study sites) and the Mauna Loa Observatory, Hawaii, respectively.
Data collection	Four automatic weather stations were installed in the two treeline forests and above both treelines (hourly records). In each of both treeline forests, five 1.5m×0.5m litterfall traps were randomly installed to monthly collect the litterfall. Eight mature, healthy trees at each of the two treeline sites were selected and mounted with automatic dendrometers at breast height to continuously monitor stem radial growth (hourly records). In 2016-2017, 2 tree-ring cores at breast height were sampled with an increment borer for each of 30 trees (including the 8 monitored trees with dendrometers) in each of both treeline species, and annual ring width was measured with a resolution of 0.01 mm.
Timing and spatial scale	We aim to examine three key issues: 1) whether seasonal and annual stem increments typically show a lagged positive relationship to litterfall, N-return and N-resorption across the two treeline stands; 2) whether annual tree-ring width, litterfall, N-return and N-resorption all have a higher sensitivity to eCO <sub>2</sub> than to the variability of temperature, precipitation and solar radiation during 2007-2017; and if so, 3) whether similar patterns are found in longer time series of tree-ring width index during 1986-2017. To test the scalability of our observed patterns, we further examined the literature data of tree-ring width for 6 other tree species at 11 treeline sites on the Tibetan Plateau.
Data exclusions	No data were excluded from the analyses.
Reproducibility	Annual tree-ring width, annual litterfall, and annual nitrogen return and resorption all showed an increasing trend during 2007-2017, and most of the variations were explained by elevated atmospheric CO <sub>2</sub> rather than climate change. Similar patterns were found in longer time series of tree-ring width index during 1986-2017. The scalability of our observed patterns was confirmed by the literature data of 6 other tree species at 11 treeline sites over the Tibetan Plateau.
Randomization	In each of both treeline forests, five 1.5m×0.5m litterfall traps were randomly installed to monthly collect the litterfall. The 8 monitored trees with dendrometers at each of the two treeline sites were selected to represent different sizes of tree diameter.
Blinding	Blinding was not relevant to our long-term located observations and measurements with automatic instruments.
Did the study involve field work?	<input checked="" type="checkbox"/> Yes <input type="checkbox"/> No

## Field work, collection and transport

Field conditions	Two alpine treeline forests at 4300-4400 m, with annual mean air temperature of 0.6 °C - 1.1 °C, the world highest timberline.
Location	At the peak of the Sergyemla Mountains (29°36'N, 94°36'E, 4300-4400 m) in southeast Tibet, China.
Access & import/export	We are free to make 10-year observations/measurements of stem radial increment, canopy litterfall and its induced nitrogen return and resorption in two alpine treeline forests on the Tibetan Plateau.
Disturbance	No disturbance

# Reporting for specific materials, systems and methods

We require information from authors about some types of materials, experimental systems and methods used in many studies. Here, indicate whether each material, system or method listed is relevant to your study. If you are not sure if a list item applies to your research, read the appropriate section before selecting a response.

## Materials & experimental systems

n/a	Involvement in the study
<input checked="" type="checkbox"/>	<input type="checkbox"/> Antibodies
<input checked="" type="checkbox"/>	<input type="checkbox"/> Eukaryotic cell lines
<input checked="" type="checkbox"/>	<input type="checkbox"/> Palaeontology and archaeology
<input checked="" type="checkbox"/>	<input type="checkbox"/> Animals and other organisms
<input checked="" type="checkbox"/>	<input type="checkbox"/> Human research participants
<input checked="" type="checkbox"/>	<input type="checkbox"/> Clinical data
<input checked="" type="checkbox"/>	<input type="checkbox"/> Dual use research of concern

## Methods

n/a	Involvement in the study
<input checked="" type="checkbox"/>	<input type="checkbox"/> ChIP-seq
<input checked="" type="checkbox"/>	<input type="checkbox"/> Flow cytometry
<input checked="" type="checkbox"/>	<input type="checkbox"/> MRI-based neuroimaging